Proceedings of the 21st ICSMGE, Vienna, Austria, 14 – 19 June 2026. Pistrol, Adam & Schweiger (eds.)
Published by: ÖGG, Austrian Society for Geomechanics, Salzburg, Austria, ISBN 978-3-9503898-4-5
https://doi.org/10.53243/ICSMGE2026-492

Numerical study on the influence of asymmetric scour on the lateral bearing capacity of large-diameter monopiles

Ben Wu
Department of Civil and Environmental Engineering, National University of Singapore, Singapore, benwu@u.nus.edu

Siau Chen Chian
Department of Civil and Environmental Engineering, National University of Singapore, Singapore, sc.chian@nus.edu.sg

ABSTRACT: Scour is one of the critical factors affecting the lateral bearing capacity of large-diameter monopiles. Due to the influence of factors such as wave-current directionality and soil properties, scour geometry often exhibits asymmetry. However, existing *p-y* models have yet to account for the influence of asymmetric scour. In this study, the three-dimensional finite element method (FEM) is employed to investigate the impact of asymmetric scour geometries on the lateral bearing behavior of monopiles. A novel method is proposed for extracting *p-y* curves from output results. 3D FEM model is validated through comparisons with existing centrifuge tests. Subsequently, a series of parametric analyses are conducted to quantify the effects of asymmetric scour geometry. The results indicate that asymmetry in scour depth has the most significant impact on the lateral bearing capacity of monopiles, while the effects of scour width and slope are relatively minor. Based on the parametric analysis, a geometric influence factor accounting for scour asymmetry is introduced into the existing *p-y* model. The rationality of the improved model is validated by the comparisons with existing tests and simulation results.

KEYWORDS: Monopile, bearing capacity, asymmetric scour, *p-y* model, FEM.

1 INTRODUCTION

Scour, a process of localized soil erosion, frequently occurs around the monopiles of offshore structures. Currently, monopiles are the main foundation type for offshore wind turbines (OWT), typically characterized by a relatively low embedment-to-diameter ratio. Most existing studies and design approaches focus on the effects of symmetrical scour pits around monopiles (Lin et al., 2014; Lin and Wu, 2019; Wang et al., 2024). However, in marine environments, scour pits around monopiles are often asymmetrical due to variations in hydrodynamic conditions. Butch et al. (1996) observed that asymmetric scour pits exhibit deeper erosion and steeper slopes on the upstream side of the monopiles, while the downstream side typically features shallower erosion and gentler slopes. This asymmetry induces differential horizontal forces on the monopiles, resulting in significant bending deformations and moments. Moreover, under large superimposed loads, the flexural deformations of monopiles are exacerbated. Despite these critical implications, research on the effects of asymmetric scour pits on monopile behavior remains limited.

Among all design methods for laterally loaded piles, the *p-y* model is one of the most widely used and has been incorporated into the API (2011) and DNV (2011) specifications. However, the *p-y* model adopted in these specifications is based on field tests of small-diameter flexible long piles. Directly applying this model to large-diameter monopiles introduces a "size effect," manifested in the influence of monopile diameter on the initial stiffness of *p-y* curves, ultimate soil resistance, and failure modes. A series of studies have been conducted to develop *p-y* models suitable for large-diameter monopiles under various soil conditions and loading scenarios (Wang et al., 2021; Wang et al., 2022; Zhang et al., 2023). Nevertheless, only a few studies (Dai et al., 2021; Wang et al., 2023; Wang et al., 2025) have addressed scour effects, and none have considered the impact of asymmetric scour on the pile-soil interaction.

In this study, finite element models are employed to investigate the effect of asymmetric scour on the interaction between large-diameter monopiles and soil, including the ultimate soil resistance and the initial foundation reaction modulus. Through a series of parametric analyses, the variation characteristics of *p-y* curves are quantified, and existing models are improved to account for the influence of asymmetric scour. Finally, the improved model is validated using existing centrifuge tests.

2 3D FEM ANALYSIS

2.1 *3D FEM model*

The commercial finite element software PLAXIS 3D is employed to construct a horizontal bearing model for a large-diameter monopile, as shown in Figure 1. Since the asymmetry of the scour holes in the transverse direction is considered, only half of the model is simulated. For the boundary condition, all directional degrees of freedom at the bottom are fixed, while only normal degrees are constrained at the lateral edges. The global dimensions of the finite-element model are governed by the geometry of the asymmetric scour hole, the monopile diameter, and its embedded depth. The soil is discretized using tetrahedral elements, and the monopile is modelled with plate elements. To accurately simulate soil-structure interaction, interface elements with zero thickness are incorporated between the soil and monopile. A rigid plate element is affixed to the top of the monopile to apply horizontal loads. The weight of the plate element is set to zero to eliminate its effect on the lateral response of the monopile. A refined meshing strategy is adopted near the monopile and the asymmetric scour zones to enhance local resolution.

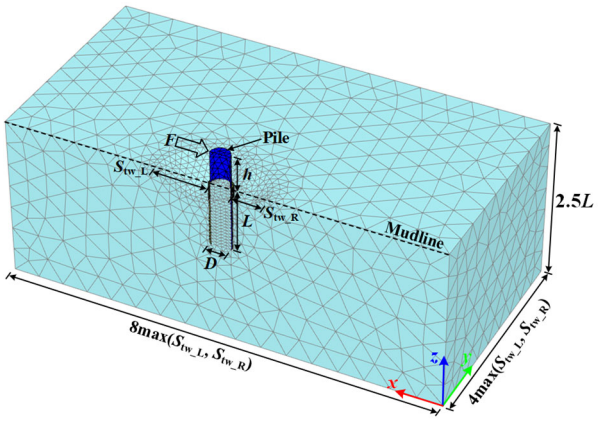

Figure 1. Geometry of finite-element model

The geometric enlargement diagram of the asymmetric scour hole is shown in Figure 2, where S_d, S_{bw}, S_{tw}, θ respectively represent the depth, bottom width, top width and slope of the scour hole, and the subscripts L and R respectively represent the left and right scour holes. To quantitatively characterize the scour hole asymmetry in terms of depth, width, and slope, the asymmetry ratio α, β, γ is introduced:

(1)

According to the geometric conditions, the relationship between the size of the scour hole is as follows:

$$S_{tw\_L} = S_{bw\_L} + S_{dL}\cot\theta_L \tag{2}$$

$$S_{tw\_R} = (\beta+1)S_{bw\_L} + (\alpha+1)S_{dL}\cot\left[(\gamma+1)\theta_L\right] \tag{3}$$

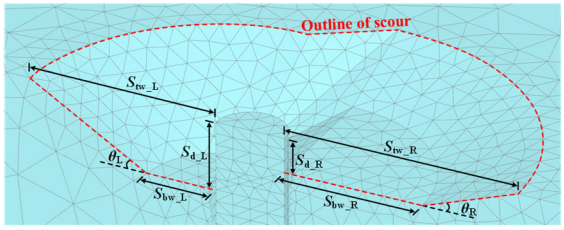

Figure 2. Geometry of asymmetric scour

2.2 *Simulation parameters*

The Hardening Soil Small-Strain (HSS) model is employed to simulate the constitutive behavior of soil. HSS model can capture the variation of soil stiffness with changes in effective stress, making it suitable for modelling soil-pile interaction (Benz, 2007). The soil constitutive model parameters utilized in this study are referenced from existing centrifuge tests (Li et al., 2024), as presented in Table 1. Elastic constitutive model is adopted for the monopile. The calculation parameters (E and υ) are also listed in Table 1. For the interface element, its strength and stiffness can be modified by the reduction coefficient R_{inter}, which is equal to 0.6-0.7 for the sand-steel interface. In this paper, R_{inter} = 0.6 is adopted (Bentley, 2022).

Table 1. Simulation parameters

Parameter	Value	Parameter	Value
γ/(kN/m^3)	15.6	υ_{ur}	0.2
c/(kPa)	0.1	p^{ref}/(kPa)	100
φ/(°)	34	K_0	0.44
ψ/(°)	4	R_f	0.9
E_{50}^{re}/(MPa)	41	G_0^{ref}/(MPa)	95.7
E_{oed}^{ref}/(MPa)	21	$\gamma_{0.7}$	0.19×10^{-3}
E_{ur}^{ref}/(MPa)	123	E/(GPa)	210
m	0.5	υ	0.3

2.3 *Generation of p-y curve in PLAXIS 3D*

Accurate derivation of p-y curve at any depth requires simultaneous determination of the lateral pile displacement y and the corresponding soil resistance p. In the post-processing system of PLAXIS 3D, y can be directly extracted from the displacement results of the plate elements, while p is not available from the standard output. The current mainstream method is to numerically differentiate the bending moment curve and then perform polynomial fitting to estimate the distribution of p. However, its accuracy depends on the smoothness of the curve and the effectiveness of the fitting algorithm. This paper presents a novel method to directly calculate soil resistance from simulation output.

In PLAXIS 3D, the stresses on interface elements consist of effective normal stress σ'_n and shear stresses τ_1, τ_2. Since τ_1 represents the shear stress along the pile axis, it is excluded from the analysis. As shown in Figure 3, the interface element is composed of triangular elements. The normal stress and shear stress are stored on the stress point of the triangular element rather than the node. Figure 4 shows the top-down view of the distribution of stress points on the interface element. For any stress point, the horizontal soil resistance can be calculated by

$$p_{ij} = \sigma'_{nij}\cos\theta_{ij} - \tau_{ij}\sin\theta_{ij} \tag{4}$$

where σ'_{nij} and τ_{ij} are the normal stress and shear stress of the stress point respectively; θ_{ij} is the angle between the connection between the stress point and the center point and the horizontal direction.

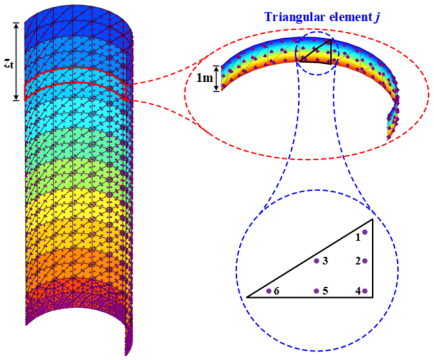

Figure 3. Distribution of stress points on interface elements

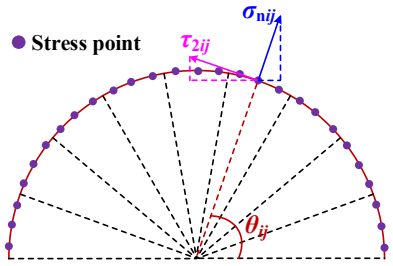

Figure 4. Calculation of soil resistance

The soil resistance at a target depth z_t can be obtained by superimposing p_{ij} of all stress points within the depth range (z_t - 1, z_t]:

$$p_{z_t} = \sum_{k=1}^{N}\sum_{i=1}^{6}\left[\sigma'_{nij}\cos\theta_{ij} - \tau_{ij}\sin\theta_{ij}\right]A_i \tag{5}$$

where N is the number of triangle units corresponding to depth z; A_i is the area corresponding to each stress point, $A_i = w_i\pi D/N$, w_i (i = 1, 2, 3, 4, 5, 6) is the weight coefficient of the stress point, refer to the PLAXIS 3D manual (Bentley, 2022).

In order to verify the accuracy of proposed method, a simplified finite element model is developed. The diameter of the monopile is 6 m, the embedded depth is 30 m, and the load eccentricity is 6 m. Figure 5 shows the comparison of the total soil resistance and the applied horizontal load under five different conditions. It can be clearly seen that the two are almost equal, with a maximum computational error of only 0.2%, proving the rationality of the proposed method.

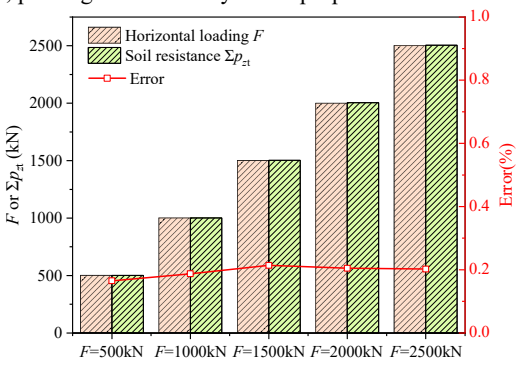

Figure 5. Validation of the calculation method of the soil resistance

2.4 *Verification of finite-element model*

Since there are few model tests and in-situ tests on asymmetric scour, the centrifuge test carried out by Li et al. (2024) of bearing capacity of pile foundation with symmetric scour is chosen to verify the proposed FEM model. The soil parameters are consistent with those listed in Table 1.

Figure 6 presents a comparison between the finite element model and the normalized *p-y* curve derived from centrifuge test results, demonstrating a high degree of agreement. Nevertheless, FEM model exhibits a slightly greater initial stiffness. This discrepancy arises because the displacement required to achieve the ultimate bearing capacity of the pile foundation in the centrifuge test is smaller than that predicted by the numerical model. Consequently, the ultimate soil resistance between the pile and the surrounding soil is not fully mobilized. Furthermore, Figure 6 illustrates that the *p-y* curve exhibits increased stiffness as the scour depth increases, underscoring the significant influence of scour depth on the bearing capacity of the monopile.

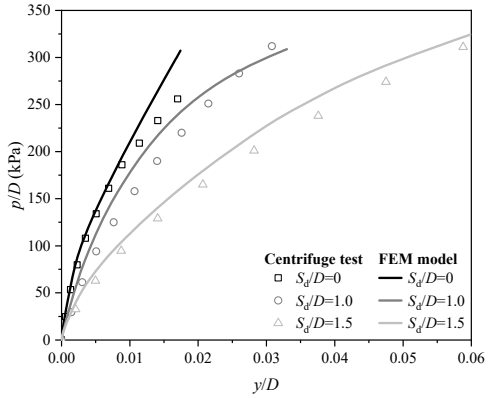

Figure 6. Comparison of normalized *p-y* curve

3 PARAMETER ANALYSIS

Based on the validated finite element model, a parametric analysis is conducted to investigate the impact of scour hole geometry on soil-pile interaction. The parameters examined include scour depth S_d, width S_b and slopeθ. To isolate the effects of individual variables, the left scour hole sizes are fixed as $S_{d\_L} = D$, $S_{bw\_L} = D$, $\theta_{\_L} = 30°$. The variation ranges for the asymmetry ratios α, β, and γ are -0.75 - 1, -0.75 - 1, and -5/6 - 0, respectively. The diameter of monopile varies from 4 m to 10 m to ensure that its stiffness meets that of rigid pile.

To characterize the *p-y* curves at different depths, absolute depth and relative depth are defined as shown in Figure 7, where MLS and MRS represent the left and right scour lines respectively. The distance from an arbitrary point to the original mudline before scouring is defined as the absolute depth z, while the ratio of the distance from an arbitrary point to the mudline after scouring to the embedded depth on the right side L' of the monopile is denoted as z'. That is $z' = [z-(\alpha+1)D]/L'$.

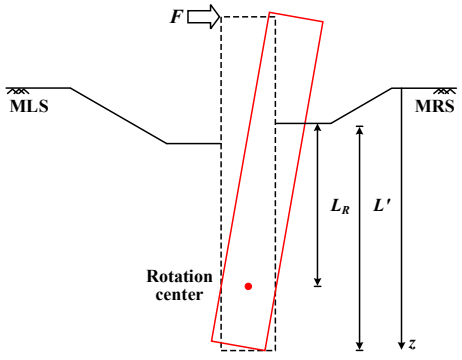

Figure 7. Definition of the relative depth z'

Figure 8(a) presents the influence of the depth asymmetry ratio α on the *p-y* curve at the same absolute depth z for D = 6 m. Although both the slope and extreme values of *p-y* curve change noticeably with α, no clear functional relationship exists between them. Specifically, the variation in *p-y* curve characteristics induced by increasing α is non-monotonic. In contrast, as shown in Figure 8(b), for *p-y* curves at identical relative depths z', the initial stiffness increases with α. A similar trend is observed for the extreme values of the curves, namely the ultimate soil resistance. This indicates that variables related to soil-pile interaction, such as soil resistance and initial foundation reaction modulus, are functions of z' rather than z.

As shown in Figures 9 and 10, the effects of width and slope asymmetry ratios β and γ are less pronounced compared to depth, differing only in ultimate soil resistance. Specifically, the ultimate soil resistance decreases with increasing β while increases with rising γ. This suggests that variations in β and γ partially alter the soil pressure distribution around the monopile, while their influence is significantly smaller than that of α. Thus, only α is considered in subsequent analyses.

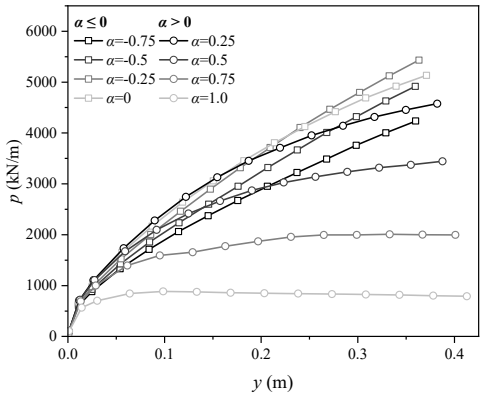

(a) Absolute depth $z = (\alpha+2)D$

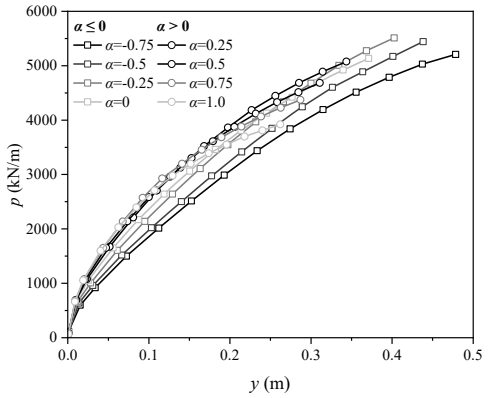

(b) Relative depth $z' = 1/3$

Figure 8. Influence of asymmetry ratio of depth α

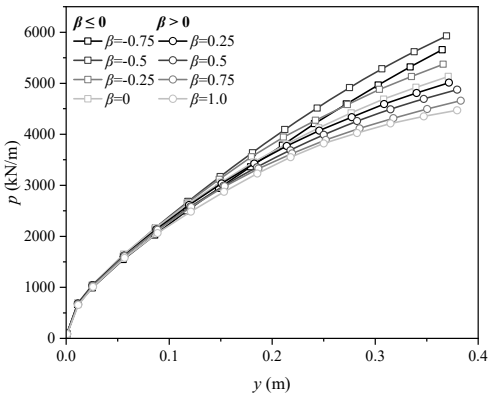

Figure 9. Influence of asymmetry ratio of width β ($z' = 1/3$)

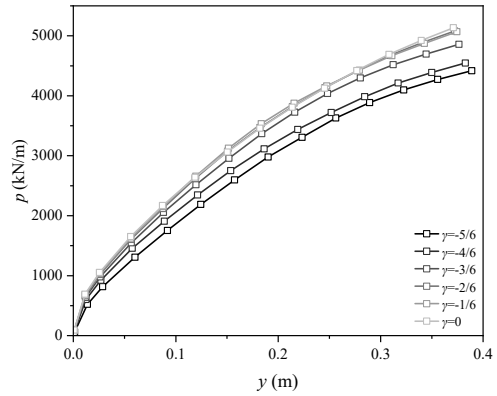

Figure 10. Influence of asymmetry ratio of slope γ ($z' = 1/3$)

4 MODIFICATION OF P-Y CURVE CONSIDERING SCOUR ASYMMETRY

Existing *p-y* models have been continuously improved for large-diameter monopiles under various soil conditions and loading conditions. However, there is still no model that considers asymmetric scour conditions. Based on the characteristics of *p-y* curves revealed in Section 3, this study improves the *p-y* curve by modifying the ultimate soil resistance p_u and initial foundation reaction modulus k, building upon the widely used hyperbolic model:

$$p = y/(1/k + y/p_u) \tag{6}$$

4.1 *Modification of the ultimate soil resistance*

Ultimate soil resistance ($p_u = K_u\sigma'_v D$) is one of the important parameters in monopile foundation design, where K_u is the ultimate soil resistance coefficient, σ'_v is the effective vertical stress, D is the monopile diameter. Current methods for K_u in sand are still not unified, and there is no algorithm specifically for asymmetric scour. Model tests carried out by Fleming et al. (2008) demonstrate that K_u is a function of the passive earth pressure coefficient K_p. This conclusion has been accepted and gradually improved. Building on this, this paper introduces a depth asymmetry influence factor δ_u, as shown in Eq. (7). By establishing the relationship between δ_u and influencing factors such as α and D, the calculation method for p_u is improved.

$$p_u = K_u\sigma'_v D = \delta_u K_p^2 \sigma'_v D \tag{7}$$

Figure 11 presents the distribution of δ_u across all parametric analysis ranges. It can be observed that despite variations in α and D, the distribution of δ_u gradually converges to a polyline. As shown in Figure 12, the polyline line characterizes the overall trend of p_u with z': it first gradually increases from δ_{u_top} to a maximum value δ_{u_max}, then decreases to zero at $z' = 0.75$ or the rotation center. Below this depth, negative soil resistance is mobilized and gradually increases to a negative extreme value δ_{u_tip} at the pile tip. Therefore, the distribution of δ_u can be represented by the following piecewise function:

$$\delta_u = \begin{cases} \dfrac{\delta_{u\_max} - \delta_{u\_top}}{z'_{max}} z' + \delta_{u\_top}, & 0 \le z' < z'_{max} \\ \dfrac{\delta_{u\_max}}{z'_{max} - 0.75}(z' - 0.75), & z'_{max} \le z' < 0.75 \\ 4\delta_{u\_tip}(z' - 0.75), & 0.75 \le z' \le 1 \end{cases} \tag{8}$$

Using the results for $D = 6$ m as a benchmark, Figure 13 shows the variation trend of each node of the piecewise function with diameter. It is evident that except for δ_{u_tip}, the node values of δ_u decrease with increasing diameter. The relative depth z'_{max} corresponding to δ_{u_max} shows the opposite trend. This highlights the significant influence of diameter on the ultimate soil resistance. Figure 13 also provides linear expressions for each node. By combining with Eq. (8), an expression for δ_u considering the depth asymmetry of the scour hole can be obtained.

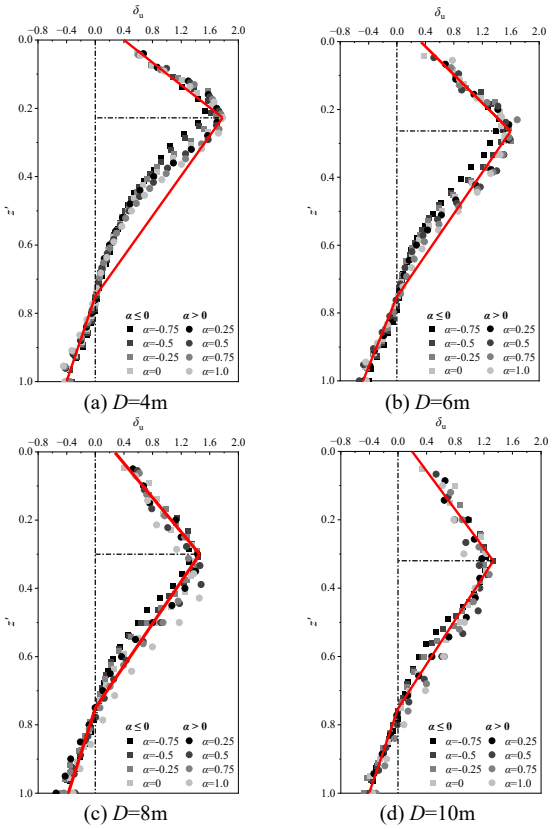

Figure 11. Combined influence of α, D and z' on the distribution of δ_u

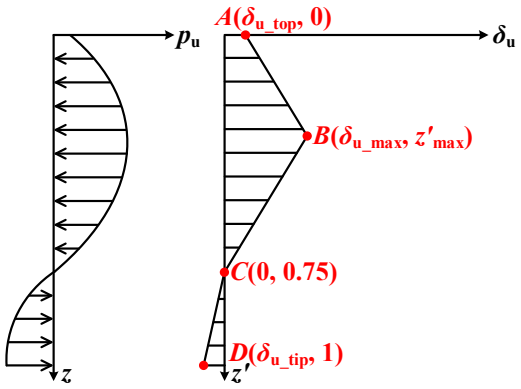

Figure 12. Illustration of calculation of δ_u

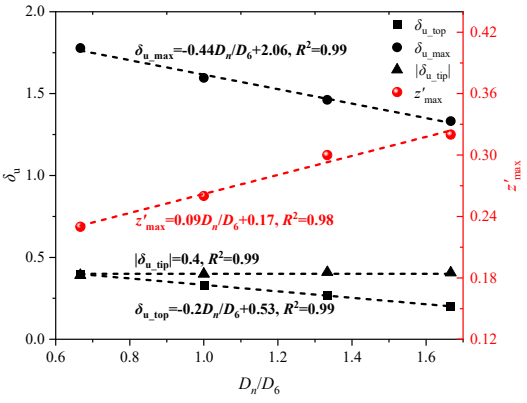

Figure 13. Variations of δ_u with increasing D_n/D_6

4.2 *Modification of the initial foundation reaction modulus*

Another important input parameter for the *p-y* curve is the initial foundation reaction modulus *k*. An accurate description of the initial segment of the *p-y* curve is crucial for calculating monopile foundation deformation and predicting natural frequencies under working loads. Similar to the ultimate soil resistance, Figure 14 presents the distribution of *k* across all parametric analysis ranges, where the solid red line is the mean line. For the same diameter *D*, α and *k* show a positive correlation, and the rate of change decreases when $\alpha > 0$. Furthermore, the distribution of *k* gradually transitions from nonlinear to linear as the diameter increases, primarily related to the pile stiffness. For non-scouring condition, Zhang et al. (2023) proposed a general expression for *k*. Based on this, this paper introduces a correction term to account for the influence of depth asymmetry, as shown in Eq. (9):

$$k = n_{\mathrm{h}} (z')^{m} \left(\frac{D}{D_6}\right)^{n} \left(\frac{\alpha+1}{\alpha_0+1}\right)^{p} \tag{9}$$

where n_{h} is the coefficient of foundation reaction, which is related to the soil density (Terzaghi, 1955); *m*, *n*, and *p* are the influence coefficients for relative depth *z'*, diameter *D*, and depth asymmetry ratio α, respectively.

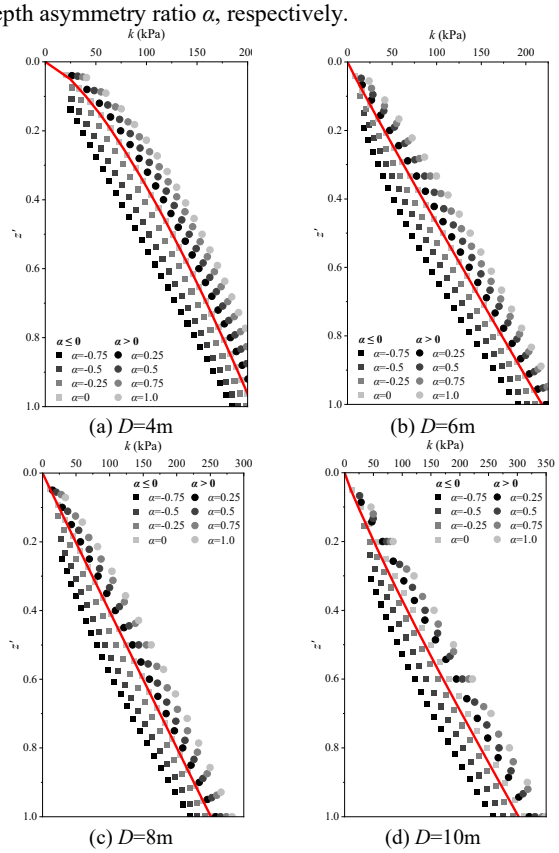

Figure 14. Combined influence of α, *D* and *z'* on the distribution of *k*

Adopting the same method used for calculating p_{u}, a certain base quantity is selected to determine the functional relationship between each influence coefficient and the relative value, as shown in Figure 15. It should be noted that although different base quantities correspond to different functional relationships, the final result of *k* is unique. Using MATLAB to perform nonlinear fitting on the data presented in Figure 15, the values of *m*, *n*, and *p* can be obtained. Substituting these into Eq. (9) yields the expression for *k*:

$$k = n_{\mathrm{h}} z' \left(\frac{D}{D_6}\right)^{0.65} \left(\frac{\alpha+1}{\alpha_0+1}\right)^{0.35} \tag{10}$$

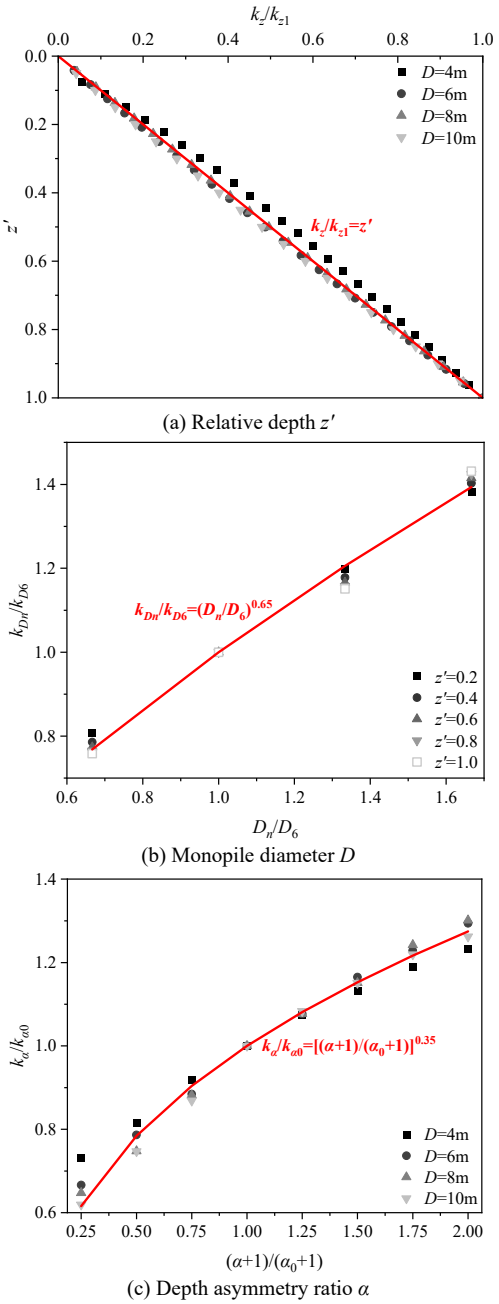

Figure 15. Variations of relative value of *k*

4.3 *Verification of proposed p-y model*

The existing centrifuge test (Li et al., 2024) is selected to validate the proposed *p-y* model. The parameters and test conditions of this experiment are consistent with Section 2.4. A comparison of the *p-y* curve is shown in Figure 16. It is evident that the proposed model predicts monopile behavior more accurately than the FEM model, particularly regarding the initial foundation reaction modulus. Furthermore, the ultimate soil resistance predicted by the modified model is slightly lower than that of the FEM model. This is related to the size effect. The modified model derived from calibration data cannot be fully applied to predict the behavior of monopiles with all diameters but demonstrates good applicability for large-diameter monopiles.

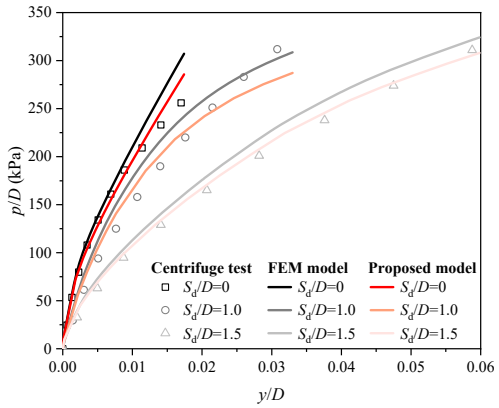

Figure 16. Verification of proposed model

5 CONCLUSIONS

This study investigates the effect of asymmetric scour on the bearing behavior of large-diameter monopiles using a finite element modeling (FEM) modeling approach. The FEM model is validated against centrifuge test results to ensure reliability. A comprehensive parametric study is carried out and reveals that asymmetric scour depth significantly influences soil-pile interaction, particularly affecting the ultimate soil resistance and initial foundation reaction modulus. In contrast, variations in scour width and slope exhibit minimal impact, causing only slight changes in ultimate soil resistance. Based on the parametric analysis results, the existing hyperbolic model is modified by introducing an influence factor for scour hole asymmetry. The modified model is validated using centrifuge tests, demonstrating good agreement with the experimental results.

6 ACKNOWLEDGEMENTS

The authors are grateful for the Ph.D. scholarship support to the first author, provided by the Singapore Ministry of Education (MOE).

7 REFERENCES

API (American Petroleum Institute). 2011. *Geotechnical and foundation design considerations*. API RP 2GEO.

Bentley (2022). *PLAXIS 3D Scientific Manual*, pp.44.

Benz, T. 2007. Small-strain stiffness of soils and its numerical consequences (Vol. 5). *Stuttgart: Univ. Stuttgart*, Inst. f. Geotechnik.

Butch, G. K. 1996. Scour-hole dimensions at selected bridge piers in New York. *In North American water and environment congress & destructive water* (pp. 3043-3051). ASCE.

Dai, S., Han, B., Wang, B., Luo, J., and He, B. 2021. Influence of soil scour on lateral behavior of large-diameter offshore wind-turbine monopile and corresponding scour monitoring method. *Ocean Engineering* 239, 109809.

DNV (Det Norske Veritas). 2011. Design of offshore wind turbine structures. *Recommended Practice DNV-RP-H103, Baerum, Norway*: Det Norske Veritas.

Fleming, K., Weltman, A., Randolph, M., and Elson, K. 2008. *Piling engineering*. CRC press.

Li, Q., Wang, X., Gavin, K., Jiang, S., Diao, H., and Wang, K. 2024. Influence of Scour Protection on the Vertical Bearing Behaviour of Monopiles in Sand. *Water* 16(2), 215.

Lin, C., Han, J., Bennett, C., and Parsons, R. L. 2014. Analysis of laterally loaded piles in sand considering scour hole dimensions. *Journal of Geotechnical and Geoenvironmental Engineering* 140(6), 04014024.

Lin, C., and Wu, R. 2019. Evaluation of vertical effective stress and pile lateral capacities considering scour-hole dimensions. *Canadian Geotechnical Journal* 56(1), 135-143.

Terzaghi, K. 1955. Evalution of conefficients of subgrade reaction. *Géotechnique* 5(4), 297-326.

Wang, H., Fraser Bransby, M., Lehane, B. M., Wang, L., and Hong, Y. 2021. Numerical investigation of the monotonic drained lateral behaviour of large-diameter rigid piles in medium-dense uniform sand. *Géotechnique* 73(8), 689-700.

Wang, H., Wang, L. Z., Askarinejad, A., Hong, Y., and He, B. 2022. Ultimate soil resistance of the laterally loaded pile in uniform sand. *Canadian Geotechnical Journal* 60(4), 587-593.

Wang, L., Wu, W., El Naggar, M. H., Zhang, Y., Liu, X., and Sun, J. 2024. Scoured failure wedge model for analysis of scoured pile-soil interaction in sand. *Computers and Geotechnics* 166, 105981.

Wang, Z., Zhou, H., Sheil, B., Liu, H., and Wang, C. 2023. Numerical investigation of the lateral response of pile groups in sand under local scour conditions. *Computers and Geotechnics* 159, 105435.

Wang, Z., Zhou, H., and Sheil, B. 2025. Effects of scour on the lateral response of piles in sand: centrifuge tests and numerical investigation. *Acta Geotechnica* 1-20.

Zhang, X. L., Zhou, R., Zhang, G. L., and Han, Y. 2023. A corrected py curve model for large-diameter pile foundation of offshore wind turbine. *Ocean Engineering* 273, 114012.